

Provided for non-commercial research and education use.
Not for reproduction, distribution or commercial use.



This article appeared in a journal published by Elsevier. The attached copy is furnished to the author for internal non-commercial research and education use, including for instruction at the authors institution and sharing with colleagues.

Other uses, including reproduction and distribution, or selling or licensing copies, or posting to personal, institutional or third party websites are prohibited.

In most cases authors are permitted to post their version of the article (e.g. in Word or Tex form) to their personal website or institutional repository. Authors requiring further information regarding Elsevier's archiving and manuscript policies are encouraged to visit:

<http://www.elsevier.com/copyright>



Field emission properties of carbon nanotube cathodes produced using composite plating

Fang-Hsing Wang^{a,*}, Tzu-Ching Lin^{a,b}, Shien-Der Tzeng^{a,c}, Ching-Tien Chou^a

^a Department and Institute of Electrical Engineering, National Chung Hsing University, 250, Kuo-Kuang Rd. Taichung 40227, Taiwan

^b Department of Electronic Engineering, National Taiwan University of Science and Technology, Taipei 106, Taiwan

^c Department of Physics, National Dong Hwa University, Hualien 974, Taiwan

ARTICLE INFO

Article history:

Received 8 January 2010

Received in revised form 12 May 2010

Accepted 6 June 2010

Available online 11 June 2010

Keywords:

Carbon nanotube(CNT)

Field emission

Composite plating

pH value

ABSTRACT

Field emission properties of carbon nanotube field emission cathodes (CNT-FECs) produced using composite plating are studied. The experiment uses a CNT suspension and electroless Ni plating bath to carry out composite plating. The CNTs were first purified by an acid solution, dispersed in a Ni electrobath, and finally co-deposited with Ni on glass substrates to synthesize electrically conductive films. Field emission scanning electron microscopy and Raman spectroscopy results show that the field emission characteristics and graphitic properties of CNT-FECs depend on the pH value of the electrobath. Experiments show that the optimum electrobath pH value is 5.4, achieving a field emission current density of 1.0 mA/cm² at an applied electric field of 1.5 V/μm. The proposed CNT-FECs possess good field emission characteristics and have potential for backlight unit application in liquid crystal displays.

© 2010 Elsevier B.V. All rights reserved.

1. Introduction

Since the landmark paper by Iijima on carbon nanotubes (CNTs) in 1991 [1], researchers have extensively investigated CNT synthesis and developed many methods of fabricating CNTs. Current CNT applications include electron field emitters, energy storage and energy conversion devices, sensors, hydrogen storage media, and nanometer-sized semiconductor devices, probes, and interconnects [2–9]. Field emitter applications, in particular, require a high aspect ratio, nano-scale diameter, high mechanical strength, and high chemical stability [10]. As a result, many researchers regard CNTs as one of the best materials for field emitters due to their singularity properties [11]. Due to their low threshold voltage, high emission current, and large field enhancement factors, CNTs are currently attracting a lot of attention for use in field emission cathodes [3–7].

Carbon nanotube field emission cathodes (CNT-FEC) could be fabricated using many methods, including direct growth [12], electrophoresis [13,14], screen-printing [4,15] and spraying [16]. Directly growing CNTs by chemical vapor deposition (CVD) [17] or arc deposition [18] requires a high deposition temperature, which limits the size and materials of the substrate. The electrophoresis method, which involves a CNT suspension, is impractical for mass production due to weak adhesion between CNTs and a sub-

strates. Screen-printing CNT films offer advantages of low cost and simplicity when used for large-sized displays. However, the screen-printing yields a poor electron field emission due to the surface modification of CNTs and entangled CNT bundles. Spraying is an easy way to deposit CNTs for field emission cathodes. To enhance adhesion between CNTs and a substrate, the spraying method uses indium (In), which is costly and scarce, as a binder. In contrast, the composite plating of CNTs and Ni is a simple and convenient method of depositing CNTs for cathodes. This composite plating approach can achieve large area deposition and reduce emission tip degradation [19]. However, the hydrophobic properties of CNTs result in poor dispersion in an electrobath [20].

To overcome the problem of CNT dispersion in a Ni bath, this study performs the acid oxidation of CNT powders [21]. This experiment fabricates CNT-FECs on glass substrates using a surfactant solution, electroless Ni plating, and multiwall carbon nanotubes (MWCNTs). The following sections also study the graphite properties, micro-structure, and field emission characteristics of the resulting CNT-FECs as a function of the electrobath pH value. This paper also discusses the adhesion between the CNT-Ni composite film and the glass substrate, the uniformity of the CNT-Ni film, the emission current density of the CNT-FEC, and the luminescence of the CNT-FEC backlight.

2. Experimental

The MWCNTs synthesized by arc discharge were first acid-treated at 110 °C in an acid solution of 75% nitric acid and 25%

* Corresponding author. Tel.: +886 4 22840688x706; fax: +886 4 22851410.
E-mail address: fansen@dragon.nchu.edu.tw (F.-H. Wang).

hydrochloric acid for 24 h and then acid-oxidized in 75% nitric acid and 25% sulfuric acid for 24 h. The MWCNTs were then washed in deionized (DI) water followed by vacuum filtering with a 0.16 μm polycarbonate filter. The purified CNTs, which exhibit characteristic changes from hydrophobic to hydrophilic at the ends of the CNTs, were then dried at 120 °C. The acid-treatment process also modifies the surface of the MWCNTs slightly, enhancing interfacial adhesion between the MWCNTs and metal [22]. The MWCNTs were also etched with nitric acid and hydrochloric acid to eliminate residual metal catalyst particles [23]. This etching helps prevent side-effects originating from the metal particles in the subsequent electroless deposition [24]. A CNT suspension consisting of MWCNTs (2 mg), surfactant solution (1 mg), and DI water (10 ml) was dispersed using ultrasonication for 30 min.

Glass substrates were cleaned in an acetone bath for 15 min with ultrasonic agitation, then rinsed in DI water for 15 min, and finally etched by air plasma (Harrick Plasma, PDC-001) for 20 min. The cleaned glass substrates were sensitized in a stannous chloride (SnCl₂·H₂O) and hydrochloric acid (HCl) solution for 1 h, and then activated in palladium chloride (PdCl₂) and HCl for 1 h. The former

sensitizing process led to the adsorption of Sn²⁺ on the substrate, while the later activation process formed fine Pd particles on the substrate through the displacement reaction of Sn²⁺ with Pd²⁺.

A Ni ion plating bath was prepared by dissolving an analytical grade NiSO₄·6H₂O in D.I. water. Table 1 lists the details of processes and associated chemical solutions. All the solutions in this experiment were prepared using DI water and reagent grade chemicals. The pH value of the plating bath was adjusted to a range of 4.2–5.6 ± 0.02 by using sulfuric acid, and the plating temperature was maintained at 80 ± 1 °C. The MWCNT solution was then dropped in the plating bath and mixed well. The glass substrates with Pd particles were subsequently dipped in the bath, allowing the electroless composite plating of CNT-Ni to form a thin film at a

Table 1
Details of the process steps and associated chemical solutions.

Step	Chemical solution
Sensitization	SnCl ₂ (0.1 g/L), HCl (0.1 ml/L)
Activation	PdCl ₂ (1.4 mg/L), HCl (0.25 ml/L)
Plating	NiSO ₄ ·6H ₂ O (87 g/L)
	NaH ₂ PO ₂ ·H ₂ O (14 g/L)
	C ₂ H ₂ (COONa) ₂ ·6H ₂ O (4.1 g/L)
	C ₃ H ₄ (OH)(COOH) ₃ ·H ₂ O (2 g/L)
	Pb(CH ₃ COO) ₂ ·3H ₂ O (0.0015 g/L)
	CH ₃ COONa·3H ₂ O (30 g/L)
	D.I. water

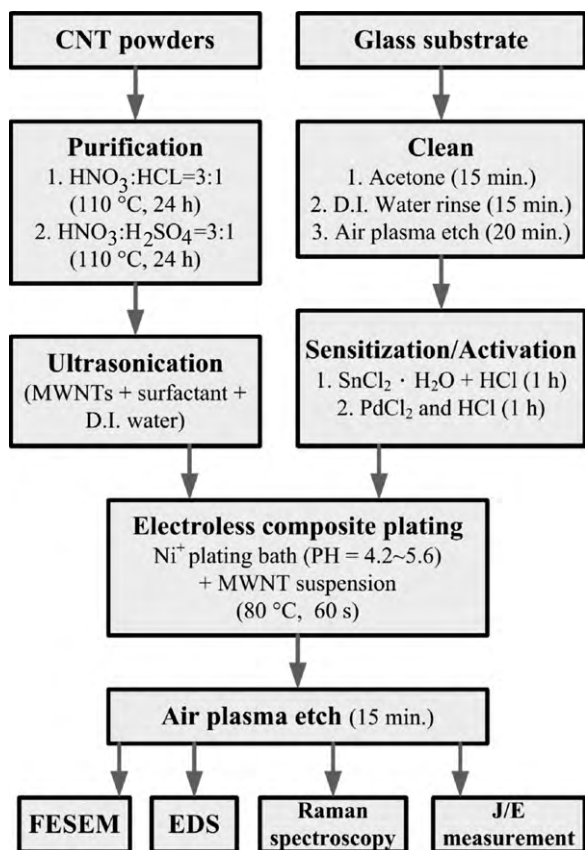


Fig. 1. The overall process flow proposed in this study.

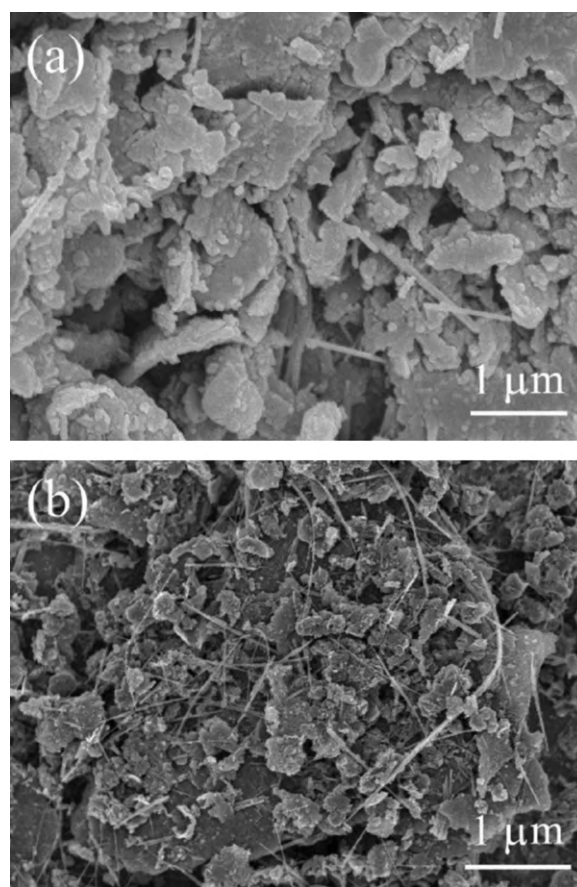


Fig. 2. FESEM images of MWCNTs: (a) pristine MWCNTs and (b) purified MWCNTs.

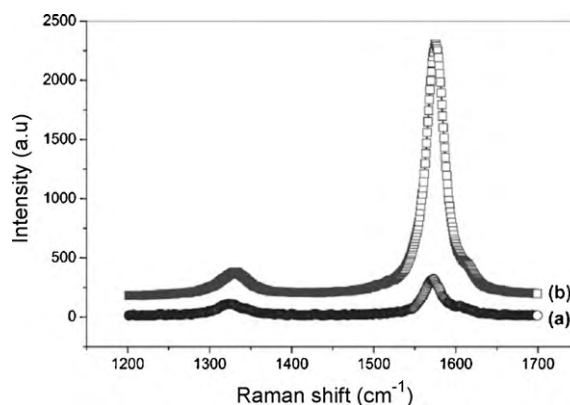


Fig. 3. Raman spectrum of MWCNTs grown by arc deposition: (a) pristine MWCNTs and (b) purified MWCNTs.

temperature of 80 °C for 60 s. After deposition, the CNT-Ni film was etched with plasma for 15 min.

The study used a field emission scanning electron microscope (FESEM, JEOL Ltd., JSM-6330) to characterize the morphology of pristine MWCNTs and CNT-Ni films. An energy dispersive X-ray spectroscope (EDS) equipped in the electron microscope analyzed the composition of the CNT-Ni films, while a Raman spectroscope (Nanofinder 30) was used to identify its structure and crystallinity. An Ar⁺ laser with a wavelength of 514.5 nm was used as the Raman excitation source. Field emission was measured with a diode structure, with indium tin oxide (ITO) glass printed with phosphor powder acting as the anode and the CNT-Ni film acting as the cathode. Field emission current densities were measured using the stand J/E measurement (Keithley 237) at a base pressure of

6×10^{-6} Torr. The gap between the sample and the anode was 80 μm . The applied voltage on the anode was increased from 0 to 1100 V at 10 V intervals. Fig. 1 depicts the entire process flow.

3. Results and discussions

Fig. 2(a) shows the FESEM image of pristine MWCNT powders made by arc discharge. The image reveals many carbon nanotubes as well as amorphous carbon and impurities. Fig. 2(b) shows the FESEM image of purified MWCNTs. Purification treatment removes oxide particles, metal particles, and non-nanotube carbon materials, and the resulting MWCNTs develop bundle structures due to strong inter-tube van der Waals interaction.

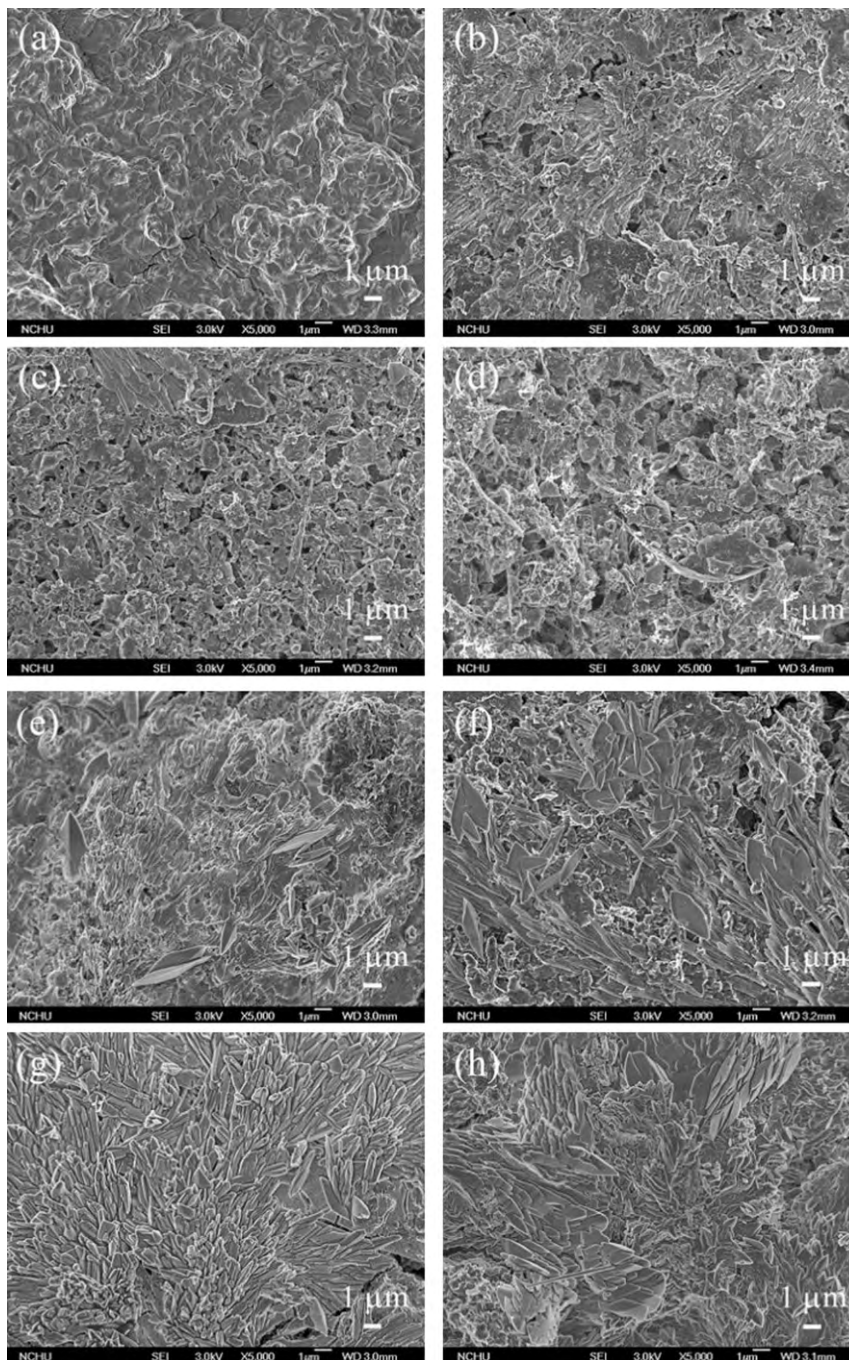


Fig. 4. FESEM images of CNT-Ni films fabricated by composite plating with various pH-value baths: (a) pH 4.2, (b) pH 4.4, (c) pH 4.6, (d) pH 4.8, (e) pH 5.0, (f) pH 5.2, (g) pH 5.4, and (h) pH 5.6.

Raman spectroscopy is one of the principal characterization techniques for studying carbonaceous materials. Fig. 3 shows the Raman spectra of the pristine MWCNTs and the purified MWCNTs. The peak at 1580 cm^{-1} corresponds to the high-frequency E_{2g} first-order mode of a graphite structure (I_G). The peak at 1350 cm^{-1} relates to the disorder of the graphite structure (I_D). The smaller the ratio of I_D to I_G , the better the graphite structure is. CNTs with high degree graphitization can improve their field emission properties [25,26]. Findings show that the ratio of I_D to I_G for the pristine MWCNTs is 0.35, whereas that for the purified MWCNTs is 0.11. A larger I_D/I_G ratio in the pristine MWCNTs reveals more defect structures in MWCNT films. In contrast, the Raman signals of the purified MWCNTs reveal fewer defects and a better graphite structure, resulting in more sp^2 bonding. The delocalized electrons in the π orbit of the sp^2 bond, which have high mobility, are more easily emitted from the CNTs than the localized electrons in σ bonds [25]. Thus, more sp^2 bonding in CNTs can improve their field emission properties [26].

Due to their strong inter-tube van der Waals attraction, MWCNTs have the propensity to aggregate into packed ropes or entangled networks. This behavior hinders the homogenous distribution of metal layers on individual nanotubes [27]. These concentric nanotubes are held together by van der Waals bonding between the layers, forming MWCNT bundles.

Fig. 4(a–h) displays the FESEM images of the CNT-Ni films fabricated by composite plating at various pH-value baths (pH 4.2–5.6). These figures show that the CNT-Ni bundles are distributed in a Ni matrix. Fig. 4(a), (b), (c) and (d) show the surfaces of the CNT cathodes plated at pH 4.2, 4.4, 4.6, and 4.8, respectively. As the pH value ranges from 4.2 to 4.8, the surface micro-structure of the CNT-Ni films becomes non-uniform and more complicated. Fig. 4(e) and (f) show that the film surfaces exhibit more CNT-Ni bundles at pH values of 5.0–5.2. As the pH value of the bath increases up to 5.4, the CNT-Ni bundles become uniform with a higher density on the surface, as Fig. 4(g) indicates. Further, Fig. 5 displays its image with higher magnification to observe the detailed morphological feature. The individual CNTs and CNT bundles were imbedded in the composite film. These results are in agreement with those reported by Wang et al. [24]. However, when the pH value further increases to 5.6, the CNT-Ni bundle phase begins to decrease.

Table 2 exhibits the compositions of the CNT-Ni films obtained by EDS analysis. As the pH value increases from 4.2 to 5.0, the carbon and Ni contents increase and the amount of other elements (phosphorous, sodium, oxygen and others) markedly decrease from 35 to 5%. Phosphorous and sodium originated from the NaH_2PO_2 used in the plating bath as a reductant of Ni. The increased Ni content indicates better electrical conductivity and the increased carbon content suggests an increased amount of MWCNTs in the plating film. When the pH value increases to 5.4, the carbon content further

Table 2

Compositions of the CNT-Ni layers fabricated by composite plating with various pH-value baths.

Element	Weight%		
	pH 4.2	pH 5.0	pH 5.4
C	55	65	70
Ni	10	30	29
Others	35	5	1
Total	100		

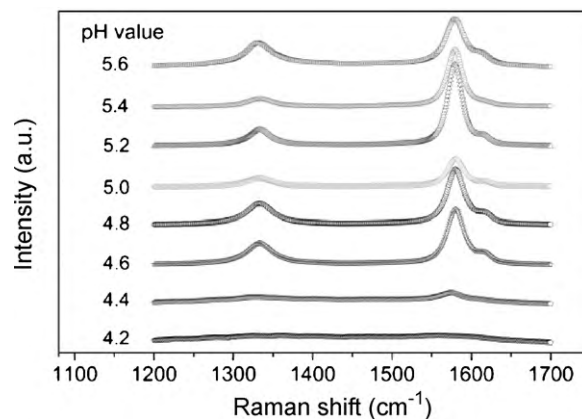


Fig. 6. Raman spectra of the CNT-Ni films as a function of plating bath pH value.

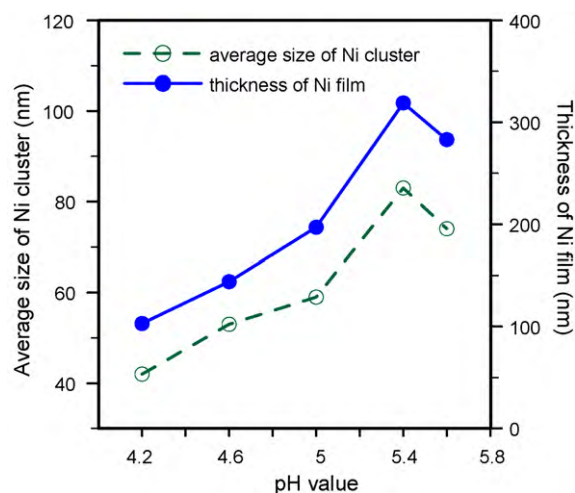


Fig. 7. Average size of Ni clusters and thickness of Ni films as a function of pH value of the plating bath.

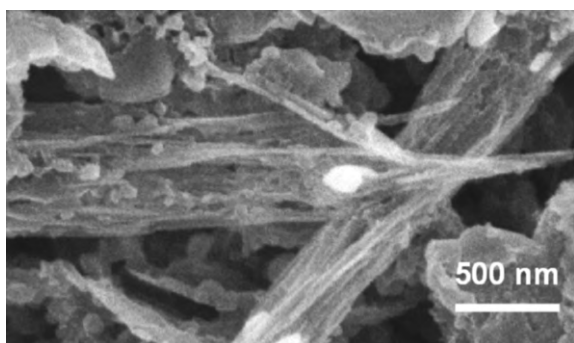


Fig. 5. FESEM image (with high magnification) of CNT-Ni films prepared by composite plating at pH 5.4.

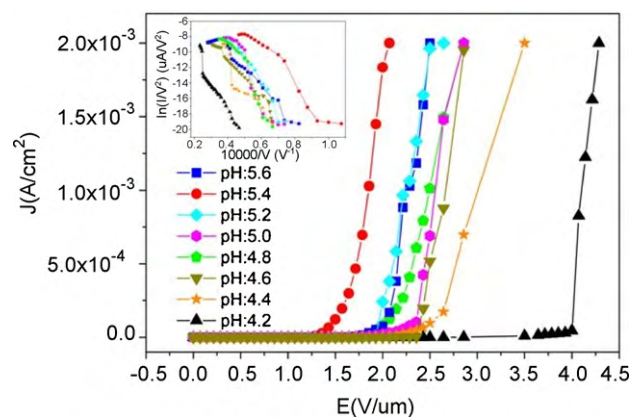


Fig. 8. Emission current densities as a function of electrical field and F-N plots (inserted) for CNT-Ni cathodes deposited with various pH-value baths.

increases up to 70% and the amount of other elements decreases to 1%. The results of the EDS analysis show that a pH value of 5.4 is optimal for composite plating, which agrees with the findings of Raman spectroscopy analysis.

Fig. 6 shows the Raman spectra of the CNT-Ni layers as a function of the pH value of the plating bath. For low pH values (4.2–4.4), the peaks at 1350 and 1580 cm^{-1} are not obvious, indicating only a few CNTs on the surface of the plating layer. As pH value of the bath continues to increase (4.6–5.0), the I_D/I_G ratio changes from 0.39 to 0.35. For high pH values of 5.2, 5.4 and 5.6, the I_D/I_G ratios

become 0.19, 0.14 and 0.18, respectively. At a pH value of 5.4, the smallest ratio of I_D to I_G reveals optimized graphitized CNTs on the CNT-Ni film. Their degree of graphitization is comparable to that of the purified CNTs, as Fig. 3 indicates. These results also agree with observations from FESEM images.

To further understand how the pH value of the plating bath influences the quality of the composite film, effects of pH value on electroless nickel plating (without CNTs), which is a similar chemical technique to the composite plating used to deposit a Ni layer. Fig. 7 exhibits the average size of Ni clusters and the thickness of Ni

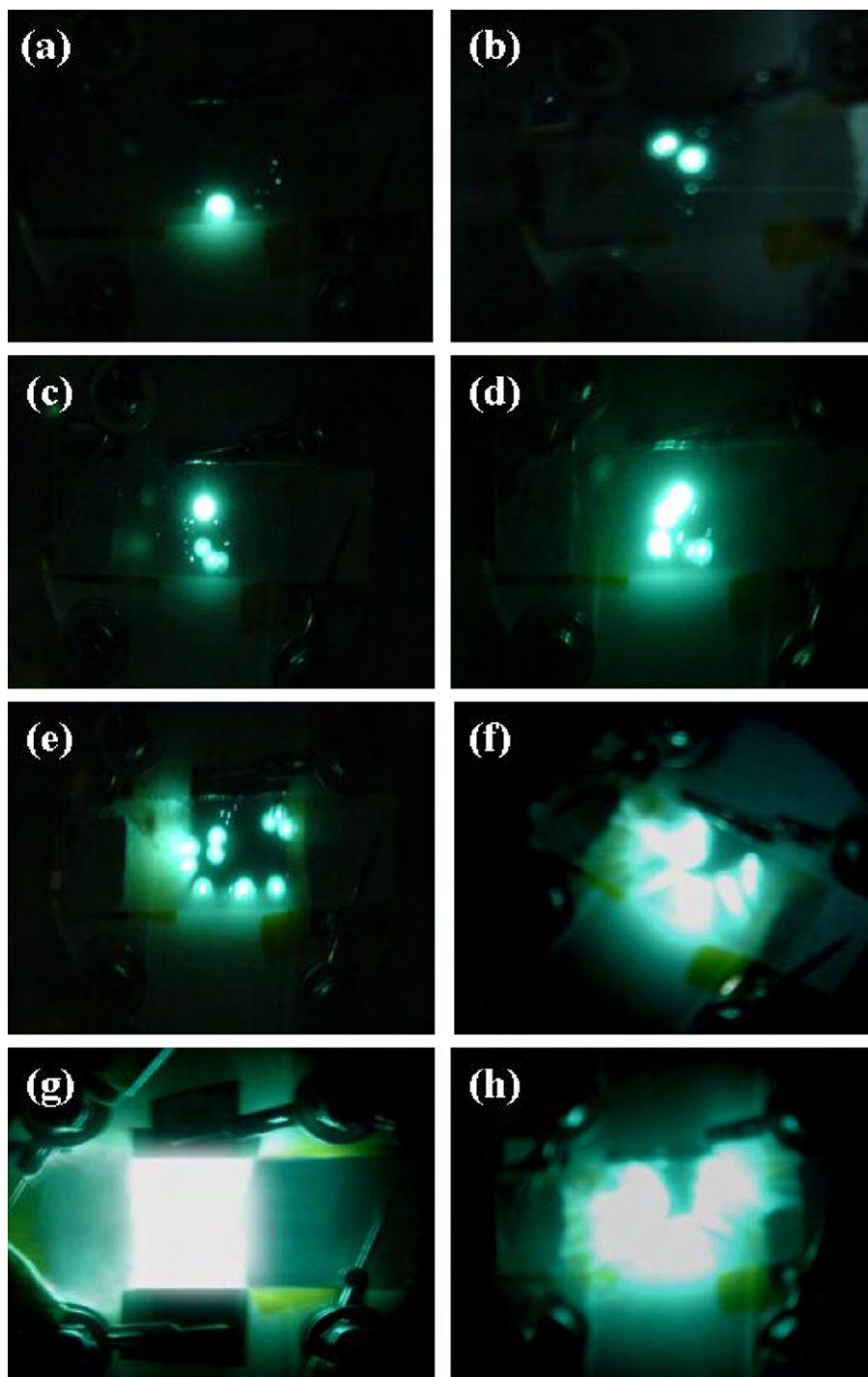


Fig. 9. Photographs of emission patterns at an applied voltage of DC 600 V for CNT-Ni cathodes fabricated with various pH-value baths: (a) pH 4.2, (b) pH 4.4, (c) pH 4.6, (d) pH 4.8, (e) pH 5.0, (f) pH 5.2, (g) pH 5.4, and (h) pH 5.6.

films prepared by electroless plating with various pH-value baths. The size of the Ni clusters and the thickness of the Ni films were obtained from plan-view and cross-section FESEM images. Findings showed that the size of the Ni clusters and the thickness of the Ni films were strongly dependent on the pH value of the plating bath. The Ni clusters were larger and the film became thicker at pH 5.4 than others. The enlarged Ni clusters and the thick Ni film indicate high deposition rate and low activation energy during electroless plating [28]. The results support that the composite-plated CNT-Ni film possesses high density of the CNT-Ni bundles and good film conductivity at pH 5.4.

To investigate the field emission characteristics of CNT-Ni films fabricated at different pH value baths, Fig. 8 shows the characteristics of emission current density vs. electric field (J - E plot) of the CNT-FECs. The figure in the insert is illustrated by Fowler-Nordheim coordinates. The turn-on electric field (E_{on}) is defined as when the emission current equals $1 \mu\text{A}$. The E_{on} nearly decreased as the pH value of the plating bath increased. The lowest E_{on} , $1.2 \text{ V}/\mu\text{m}$, appeared at a pH value of 5.4, while E_{on} was $2.8 \text{ V}/\mu\text{m}$ at pH 4.2. The threshold electric field (E_{th}) (defined as 1-mA emitted current) decreased from 4.1 to $1.5 \text{ V}/\mu\text{m}$ as the pH value increased from 4.2 to 5.4. When the pH value of the bath further increased to 5.6, the emission current of the CNT-FEC became smaller than that in a pH 5.4 bath.

The field emission data were also analyzed using the F-N model [29], (the plot of $\ln I/V^2$ vs. $1/V$). According to the F-N equation, the emission current density is the function of E , β , and ϕ : $J = A(\beta E)^2 \exp(-B\phi^3/2\beta E)$, where J is the current density, A and B are constants, E is the applied electric field, β the field enhancement factor, and ϕ is the work function of graphite [25]. Given that $\phi = 5 \text{ eV}$, the enhancement factor β increased from 1595 to 3827 when the pH value increased from 4.2 to 5.4. However, the enhancement factor decreased to 2616 as the pH value further increased to 5.6, indicating that the optimal field emission characteristic also occurs at a pH value of 5.4.

Fig. 9(a-h) shows the emission images of the CNT-FECs fabricated with different pH value baths under DC 600 V. The field strength related to these images is $7.5 \text{ V}/\mu\text{m}$. The luminescence uniformity in Fig. 9(a-e) is poor, as many sites did not light. With the pH values of 5.2 (Fig. 9(f)) and 5.6 (Fig. 9(h)), the emitted light became more uniform. However, some dark spots continued to exist in some positions, which is not acceptable in commercial displays. A uniform plane-type lighting image appeared at a pH value of 5.4, as Fig. 9(g) indicates. This superior lighting is due to the uniform distribution and high density of CNT-Ni emitters in the whole area. This means that the CNT-Ni cathode fabricated at pH 5.4 can produce better field emission characteristics and a more uniform luminescence image.

4. Conclusions

This study shows the properties of the CNT-Ni films on glass substrates fabricated by composite plating with various pH-value (4.2–5.6) baths. A pH value of 5.4 produces the most uniform and dense CNT-Ni bundles. This allows the composite plated CNT-Ni cathode to achieve a high current density and uniform luminescence. The good field emission properties and uniform luminescence of the proposed CNT-FEC are attributable to the uniform and high-density graphitized MWCNTs and good adhesion and conductivity of the CNT-Ni films. In the near future, the proposed deposition technique for CNT-FECs has potential for fabrication of backlight units in liquid-crystal displays.

Acknowledgment

The authors would like to thank the National Science Council of the Republic of China (Taiwan) for partial financial support under Contract No. NSC 95-2221-E-005-111.

References

- [1] S. Iijima, Helical microtubes of graphitic carbon, *Nature* 354 (1991) 56–58.
- [2] R.G. Ding, G.Q. Lu, Z.F. Yan, M.A. Wilson, Recent advances in the preparation and utilization of carbon nanotubes for hydrogen storage, *J. Nanosci. Nanotechnol.* 1 (2001) 7–29.
- [3] Q.H. Wang, A.A. Setlur, J.M. Lauerhaas, J.Y. Dai, E.W. Seelig, A nanotube-based field-emission flat panel display, *Appl. Phys. Lett.* 72 (1998) 2912–2913.
- [4] J.L. Kwo, M. Yokoyama, W.C. Wang, F.Y. Chuang, I.N. Lin, Characteristics of flat panel display using carbon nanotube as electro emitters, *Diam. Relat. Mater.* 9 (2000) 1270–1274.
- [5] L. Wang, Z. Sun, T. Chen, W. Que, Growth temperature effect field emission properties of printable carbon nanotubes cathode, *Solid State Electron.* 50 (2006) 800–804.
- [6] Y. Qin, M. Hu, H. Li, Z. Zhang, Q. Zou, Preparation and field emission properties of carbon nanotubes cold cathode using melting Ag nano-particles as binder, *Appl. Surf. Sci.* 253 (2007) 4021–4024.
- [7] A. Schindler, J. Brill, N. Fruehauf, J.P. Novak, Z. Yaniv, Solution-deposited carbon nanotube layers for flexible display applications, *Physica E* 37 (2007) 119–123.
- [8] C. Niu, E.K. Sichel, R. Hoch, D. Moy, H. Tennent, High power electrochemical capacitors based on carbon nanotube electrodes, *Appl. Phys. Lett.* 70 (1997) 1480–1482.
- [9] J. Kong, N.R. Franklin, C. Zhou, M.G. Chapline, S. Peng, K. Cho, H. Dai, Nanotube molecular wires as chemical sensors, *Science* 287 (2000) 622–625.
- [10] M. Hirakawa, S. Sonoda, C. Tanaka, H. Murakami, H. Yamakawa, Electron emission properties of carbon nanotubes, *Appl. Surf. Sci.* 169–170 (2001) 662–665.
- [11] W.A. Deheer, A. Chatelain, D. Ugarte, A carbon nanotube field-emission electron source, *Science* 75 (1995) 129–131.
- [12] Z.F. Ren, Z.P. Huang, J.W. Xu, J.H. Wang, P. Bush, M.P. Siegal, P.N. Provencio, Synthesis of large arrays of well-aligned carbon nanotubes on glass, *Science* 282 (1998) 1105–1107.
- [13] L.M. Yu, C.C. Zhu, Field emission characteristics study for ZnO/Ag and ZnO/CNTs composites produced by DC electrophoresis, *Appl. Surf. Sci.* 255 (2009) 8359–8362.
- [14] Y. Qin, M. Hu, Field emission properties of electrophoretic deposition carbon nanotubes film, *Appl. Surf. Sci.* 255 (2009) 7618–7622.
- [15] F.G. Zeng, C.C. Zhu, W. Liu, X. Liu, The fabrication and operation of fully printed Carbon nanotube field emission displays, *Microelectron. J.* 37 (2006) 495–499.
- [16] Y.D. Lee, K.S. Lee, Y.H. Lee, B.K. Ju, Field emission properties of carbon nanotube film using a spray method, *Appl. Surf. Sci.* 254 (2007) 513–516.
- [17] Z.W. Pan, S.S. Xie, B.H. Chang, L.F. Sun, W.Y. Zhou, G. Wang, Direct growth of aligned open carbon nanotubes by chemical vapor deposition, *Chem. Phys. Lett.* 299 (1999) 97–102.
- [18] P.M. Ajayan, S. Iijima, Capillarity-induced filling of carbon nanotubes, *Nature* 361 (1993) 333–334.
- [19] Y.M. Liu, Y. Sung, Y.C. Chen, C.T. Lin, Y.H. Chou, M.D. Ger, A method to fabricate field emitters using electroless codeposited composite of MWCNTs and nickel, *Electrochem. Solid State Lett.* 10 (2007) J101–104.
- [20] D.O. Kim, M.H. Lee, J.H. Lee, T.W. Lee, K.J. Kim, Y.K. Lee, T. Kim, H.R. Choi, J.C. Koo, J.D. Nam, Transparent flexible conductor of poly(methyl methacrylate) containing highly-dispersed multiwalled carbon nanotube, *Org. Electron.* 9 (2008) 1–13.
- [21] S. Ravindran, S. Chaudhary, B. Colburn, M. Ozkan, C.S. Ozkan, Covalent coupling of quantum dots to multiwalled carbon nanotubes for electronic device applications, *Nano Lett.* 3 (2003) 447–453.
- [22] K. Esumi, M. Ishigami, A. Nakajima, K. Swada, H. Honda, Chemical treatment of carbon nanotubes, *Carbon* 34 (1996) 279–281.
- [23] Y. Zhang, Z. Shi, Z. Gu, S. Iijima, Structure modification of singlewall carbon nanotubes, *Carbon* 38 (2000) 2005–2009.
- [24] F. Wang, S. Arai, M. Endo, The preparation of multi-walled carbon nanotubes with a Ni-P coating by an electroless deposition process, *Carbon* 43 (2005) 1716–1721.
- [25] S. Han, J. Ihm, Role of the localized states in field emission of carbon nanotubes, *Phys. Rev. B* 61 (2000) 9986–9989.
- [26] K.F. Chen, K.C. Chen, Y.C. Jiang, L.Y. Jiang, Y.Y. Chang, M.C. Hsiao, L.H. Chan, Field emission image uniformity improvement by laser treating carbon nanotube powders, *Appl. Phys. Lett.* 88 (2006) 193127–193128.
- [27] C.Y. Zhi, X.D. Bai, E.G. Wang, Enhanced field emission from carbon nanotubes by hydrogen plasma treatment, *Appl. Phys. Lett.* 81 (2002) 1690–1692.
- [28] W.L. Liu, S.H. Hsieh, T.K. Tsai, W.J. Chen, S.S. Wu, Temperature and pH dependence of the electroless Ni-P deposition on silicon, *Thin Solid Films* 510 (2006) 102–106.
- [29] R.H. Fowler, L.W. Nordheim, Electron emission in intense electric fields, *Proc. R. Soc. Lond. Ser. A* 119 (1928) 173–181.